International Core Journal of Engineering Volume 7 Issue 7, 2021
ISSN: 2414-1895 DOI: 10.6919/ICJE.202107_7(7).0050

Geometric Nonlinear Analysis of Floating Crane Based on Finite Particle Method

Jiaming Pu, Long Liu and Chen Nan

Shanghai Offshore Engineering Research Institute, Shanghai Maritime University, Shanghai 201306, China.

Abstract

Based on the beam element theory of finite particle method, a 7000 t floating crane is selected for analysis. Considering the initial deformation caused by the gravity, the load-displacement curve of the crane in particular working condition is calculated and analyzed, and the geometric nonlinear process are tracked to obtain the ultimate load and instability state. The accuracy of this new method is verified by comparing the analysis results of the Matlab program with APDL, which provides a reference for the stability design of the crane in practical engineering.

Keywords

Floating Crane; Finite Particle Method; Stability Analysis; Geometric Nonlinear Analysis.

1. Introduction

With the increasing of port cargo throughput, the lifting machinery develops towards large and towering direction. However, the nonlinear effect of crane in complex working environment is more and more prominent. Its load is complex and changeable, and the dynamic characteristic is remarkable. So as the whole crane metal skeleton structure, the design and manufacture quality will directly affect the whole crane technical and economic index.

Floating crane is mainly steel structure, the past scholars have done a lot of research on the stability of steel structure. Yurchenko D. and Alevras P.[1] investigated stochastic dynamics and stability of a ship-based crane, and considered the simplified nonlinear model of the payload motion, where the excitation of a suspension point was imposed due to heaving motion of waves. Jung Hoon-Hyung and Kim Chae-Sil[2] described a finite element structural analysis model and determined analysis methods appropriate for determining the stability of the mast of a crane. Wenjun Li et al.[3] carried out a dually nonlinear buckling analysis on flexible giant crane boom. The incremental load method, the incremental displacement method, and the Newton-Raphson method were applied to obtain the load-deflection response and the critical load. The survey results were used to varified the numerical analysis. Simao Pedro D.[4] dealed with buckling aspects of the design of stepped columns in mill buildings, and presented a discussion on the variation of the load carrying capacity with the level of eccentricity and lateral load acting at the step on a practical column. Jia Yao et al.[5] carried out the Finite Element Analysis (FEA) to investigate the failure reason of an all-terrain crane telescopic boom, and used the nonlinear static method and explicit dynamic method to study the boom buckling failure and stress wrinkle. In order to analyze the stress levels nearby the failure region and to discuss the fatigue design with reference to current standards, Frendo Francesco[6] discussed the catastrophic failure of a crane jib, and carried out a stress analysis of the crane jib..

The FEM(Finite Element Method) still has its limitation for the problem of large deformation and displacement, and it is very expensive for the nonlinear analysis of complex structures. The VFIFE(Vector Form Intrinsic Finite Element) is a new mechanical calculation method proposed by professor Ding Chengxian[7], it combins the concepts of vector mechanics and FEM, which can

ISSN: 2414-1895 DOI: 10.6919/ICJE.202107_7(7).0050

effectively solve the complex mechanical behaviors of structures, such as elastoplastic, buckling instability, collision and collapse. For more than ten years, Luo Yaozhi's[8] team has been conducting in-depth research towards practical engineering structure applications. According to the characteristics of this method, it has been named FPM(Finite Particle Method). They also developed an platform based on FPM. Yan Zhang et al.[9] proposed an effective computational method for the non-prestressed cable net structure with large deformation problem, and analyzed the numerical examples such as the rod chain mechanism and the space hyperboloid cable net, which verified the feasibility and correctness of this method. Yu Ying and Xingyi Zhu[10] developed the fracture criterion and fracture model of the FPM,and considered the influence of nonlinear and hysteretic connection stiffness, they also analyzed the collapse of a Vogel six-story frame. Yulong Yang et al.[11] developed a joint model to simulate the motion of multibody systems, and analyzed the dynamic behaviour of a four-bar mechanism with three joins. Jingzhe Tang et al.[12] proposed a GPU-accelerated parallel strategy for the FPM, evaluated and assembled the element equivalent forces and solved the kinematic equations through careful thread management and memory optimization performance. Feihong Liu et al.[13] proposed an efficient numeric approach coupling smoothed particle hydrodynamics(SPH) with FPM for fluid-interaction problems.Yuanfeng Duan et al.[14] introduced VFIFE analysis to a real-time hybrid simulation with numerical substructures containing a large number of DOFs.

Based on the three-dimensional beam element theory of FPM, this paper carries out a static analysis on the crane and compares with the results of ANSYS. After the buckling and instability analysis of the structure, the load-displacement curve of the boom is obtained, so as to understand the influence of each component of the structure on the overall stability, which provides a reference for engineering design.

2. Finite Particle Method

The FPM includes three basic concepts: point value description, path element and reverse motion. Firstly, the geometrical shape and spatial position of the structure are described by the spatial and temporal trajectories of a finite particles. All the mass, displacement, deformation, boundary conditions, internal and external forces on the structure are assumed by the particles. Secondly, the motion of particles are controlled by Newton's law of motion, and the pure deformation is obtained by using the virtual reverse motion to calculate the internal force. In order to satisfy the hypothesis of small deformation in material mechanics, the motion and deformation of the structure in a period of time are divided into several path units of micro time segments. Finally, the calculation of motion and deformation is realized through continuous updating and iteration.

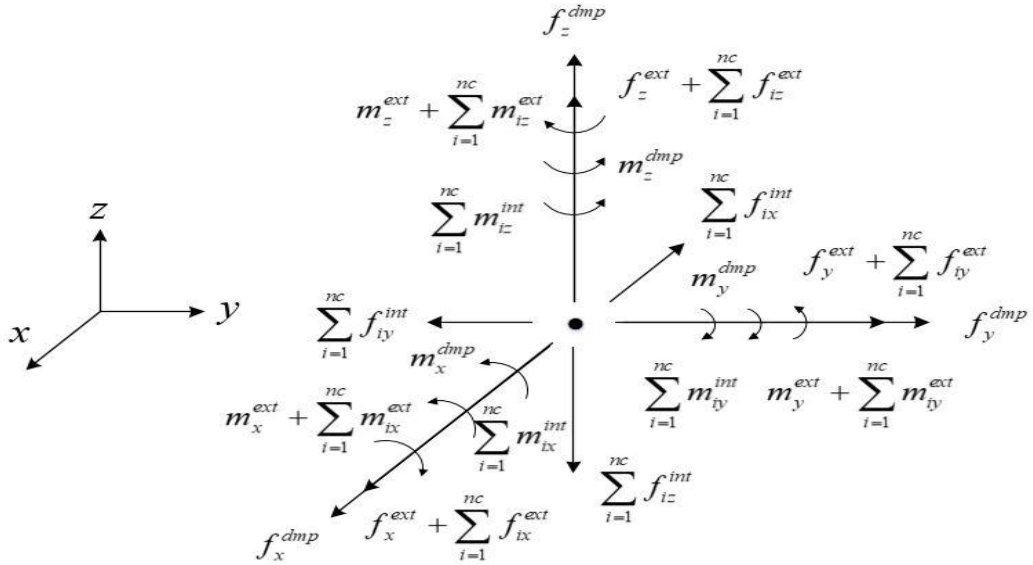

Figure 1. Particle forces and moments of space beam elements

ISSN: 2414-1895 DOI: 10.6919/ICJE.202107_7(7).0050

Compared with the FEM, the FPM is suitable for solving both static and dynamic problems. The update of the reference configuration automatically meets the requirements of incremental analysis, and it can be used to analyze geometric nonlinear problems without any other modification in the calculation format.

2.1 Governing Equation

The research object of the FEM is a series of spatial particles describing the structure, so its governing equation is a set of point motion formulas obtained by Newton's law of motion, and solved by explicit central difference method.

Translational and rotational differential equations of a single particle is:

$$M_\alpha \frac{\mathrm{d}^2}{\mathrm{d}t^2}\begin{bmatrix} d_x \\ d_y \\ d_z \end{bmatrix}_\alpha = \begin{bmatrix} f_x^{ext} + \sum_{i=1}^{nc} f_{ix}^{ext} \\ f_y^{ext} + \sum_{i=1}^{nc} f_{iy}^{ext} \\ f_z^{ext} + \sum_{i=1}^{nc} f_{iz}^{ext} \end{bmatrix}_\alpha - \begin{bmatrix} \sum_{i=1}^{nc} f_{ix}^{int} \\ \sum_{i=1}^{nc} f_{iy}^{int} \\ \sum_{i=1}^{nc} f_{iz}^{int} \end{bmatrix}_\alpha + \begin{bmatrix} f_x^{dmp} \\ f_y^{dmp} \\ f_z^{dmp} \end{bmatrix}_\alpha \quad (1)$$

$$\mathbf{I}_\alpha \frac{\mathrm{d}^2}{\mathrm{d}t^2}\begin{bmatrix} \theta_x \\ \theta_y \\ \theta_z \end{bmatrix}_\alpha = \begin{bmatrix} m_x^{ext} + \sum_{i=1}^{nc} m_{ix}^{ext} \\ m_y^{ext} + \sum_{i=1}^{nc} m_{iy}^{ext} \\ m_z^{ext} + \sum_{i=1}^{nc} m_{iz}^{ext} \end{bmatrix}_\alpha - \begin{bmatrix} \sum_{i=1}^{nc} m_{ix}^{int} \\ \sum_{i=1}^{nc} m_{iy}^{int} \\ \sum_{i=1}^{nc} m_{iz}^{int} \end{bmatrix}_\alpha + \begin{bmatrix} m_x^{dmp} \\ m_y^{dmp} \\ m_z^{dmp} \end{bmatrix}_\alpha \quad (2)$$

Where M_α is the mass of particle α; $[\boldsymbol{d_x} \quad \boldsymbol{d_y} \quad \boldsymbol{d_z}]_{\boldsymbol{\alpha}}^{\boldsymbol{T}}$ are the axial displacement vector of the particle; $\left[\boldsymbol{f_x^{ext}} \quad \boldsymbol{f_y^{ext}} \quad \boldsymbol{f_z^{ext}}\right]_{\boldsymbol{\alpha}}^{\boldsymbol{T}}$ are a vector of concentrated external forces acting directly on particle α; $\left[\boldsymbol{f_{ix}^{ext}} \quad \boldsymbol{f_{iy}^{ext}} \quad \boldsymbol{f_{iz}^{ext}}\right]_{\boldsymbol{\alpha}}^{\boldsymbol{T}}$ and $\left[\boldsymbol{f_{ix}^{int}} \quad \boldsymbol{f_{iy}^{int}} \quad \boldsymbol{f_{iz}^{int}}\right]_{\boldsymbol{\alpha}}^{\boldsymbol{T}}$ are respectively the equivalent external force vector and the internal force vector provided by the beam element *i* connected with the particle α; $\left[\boldsymbol{f_x^{dmp}} \quad \boldsymbol{f_y^{dmp}} \quad \boldsymbol{f_z^{dmp}}\right]_{\boldsymbol{\alpha}}^{\boldsymbol{T}}$ are the damping force vector acting on the particle α; nc is the number of beam elements connected to the particle; I_α is the mass moment of inertia matrix of particle α; $[\boldsymbol{\theta_x} \quad \boldsymbol{\theta_y} \quad \boldsymbol{\theta_z}]_{\boldsymbol{\alpha}}^{\boldsymbol{T}}$ are the axial rotation angle vector of the particle; $\left[\boldsymbol{m_x^{ext}} \quad \boldsymbol{m_y^{ext}} \quad \boldsymbol{m_z^{ext}}\right]_{\boldsymbol{\alpha}}^{\boldsymbol{T}}$ are the external concentrated moment vector acting directly on the particle α; $\left[\boldsymbol{m_{ix}^{ext}} \quad \boldsymbol{m_{iy}^{ext}} \quad \boldsymbol{m_{iz}^{ext}}\right]_{\boldsymbol{\alpha}}^{\boldsymbol{T}}$ and $\left[\boldsymbol{m_{ix}^{int}} \quad \boldsymbol{m_{iy}^{int}} \quad \boldsymbol{m_{iz}^{int}}\right]_{\boldsymbol{\alpha}}^{\boldsymbol{T}}$ are respectively the equivalent external moment vector and internal moment vector provided by the beam element *i* connected to the particle; $\left[\boldsymbol{m_x^{dmp}} \quad \boldsymbol{m_y^{dmp}} \quad \boldsymbol{m_z^{dmp}}\right]_{\boldsymbol{\alpha}}^{\boldsymbol{T}}$ are the damping moment vector acting on the particle α.

Explicit central difference method is used to solve the motion equation iteratively:

$$\ddot{d} = \frac{1}{h^2}(d_{n+1} - 2d_n + d_{n-1}) \quad (3)$$

$$\ddot{\theta} = \frac{1}{h^2}(\theta_{n+1} - 2\theta_n + \theta_{n-1}) \quad (4)$$

Where subscripts n, $n+1$ and $n-1$ are step numbers; h is the iteration step length; $\ddot{d}$ and d are the acceleration vector and displacement vector of the particle respectively; $\ddot{\theta}$ and θ are respectively the angular accleration vector and the rotation angle vector of the particle. After the initial conditions of the particle state are obtained, the central difference method can be iterated continuously and the motion and deformation of the structure at each moment can be calculated.

2.2 Reverse Translation

Selecting a beam element to move from $t_a \le t \le t_b$ along the path element. The geometry of the beam is determined by a line defined by two nodes, numbered $(1,2)$ at time t and $(1_a, 2_a)$ at time t_a respectively. The shape of the unit, the location of the node, the internal forces and the properties of the material at the time t_a are all known. The $1_a, 2_a$ node position vector of the time t_a is d_{1a}, d_{2a}, and the principal axis direction is $\boldsymbol{e}_a$, then the $1,2$ node position vector of the time t is

ISSN: 2414-1895 DOI: 10.6919/ICJE.202107_7(7).0050

d_{1t}, d_{2t}, and the principal axis direction is $\boldsymbol{e}_t$. From t_a to t, the displacement and rotation angle of the node are:

$$\begin{cases} \mathbf{u}_{1t} = \mathrm{d}_{1t} - \mathrm{d}_{1a} \\ \mathbf{u}_{2t} = \mathrm{d}_{2t} - \mathrm{d}_{2a} \\ \theta_1 = \theta_{1t} - \theta_{1a} \\ \theta_2 = \theta_{2t} - \theta_{2a} \end{cases} \tag{5}$$

The displacement of beam element node is divided into translation and rotation. Let the displacement increment of node 1 be the translation of the beam element. Through reverse translation, node 1 and 1_a are merged together, as shown in Figure 1. Obtaining the relative displacement vector of nodes 1 and 2 to the reference point node 1 :

$$\begin{cases} \boldsymbol{\eta}_1^t = 0 \\ \boldsymbol{\eta}_2^t = \mathbf{u}_{2t} - \mathbf{u}_{1t} \end{cases} \tag{6}$$

The rotation angle of the beam element is determined by the angle θ between the principal axis direction $\boldsymbol{e}_t$ at time t and the principal axis direction $\boldsymbol{e}_a$ at time t_a.

$$\theta = sin^{-1}(|\mathbf{e}_a \times \mathbf{e}_t|) \tag{7}$$

The direction of rotation axis is :

$$\boldsymbol{e}_{at} = \frac{\boldsymbol{e}_a \times \boldsymbol{e}_t}{|\boldsymbol{e}_a \times \boldsymbol{e}_t|} \tag{8}$$

The node displacement caused by the rotation of beam element is :

$$\begin{cases} \boldsymbol{\eta}_1^r = 0 \\ \boldsymbol{\eta}_2^r = \boldsymbol{R}^*(\boldsymbol{x}_{2t} - \boldsymbol{x}_{1t}) \end{cases} \tag{9}$$

$$\mathbf{R}^* = [1 - cos(-\theta)]\mathbf{A}^2 + sin(-\theta)\,\mathbf{A} \tag{10}$$

Equation (10) is the transformation form of Rodrigues' rotation formula. The matrix $\boldsymbol{A}$ is a rotation matrix composed of uint rotation axis direction vectors. If $\boldsymbol{e}_{at} = [l \quad m \quad n]^T$, then

$$\mathbf{A} = \begin{bmatrix} 0 & -n & m \\ n & 0 & -l \\ -m & l & 0 \end{bmatrix} \tag{11}$$

Therefore, the total relative displacement of the node caused by translation and rotation is (the reference point is node 1)

$$\begin{cases} \boldsymbol{\eta}_1 = 0 \\ \boldsymbol{\eta}_2 = \boldsymbol{\eta}_2^t + \boldsymbol{\eta}_2^r = \boldsymbol{u}_{2t} - \boldsymbol{u}_{1t} + \boldsymbol{R}^*(\boldsymbol{x}_{2t} - \boldsymbol{x}_{1t}) \end{cases} \tag{12}$$

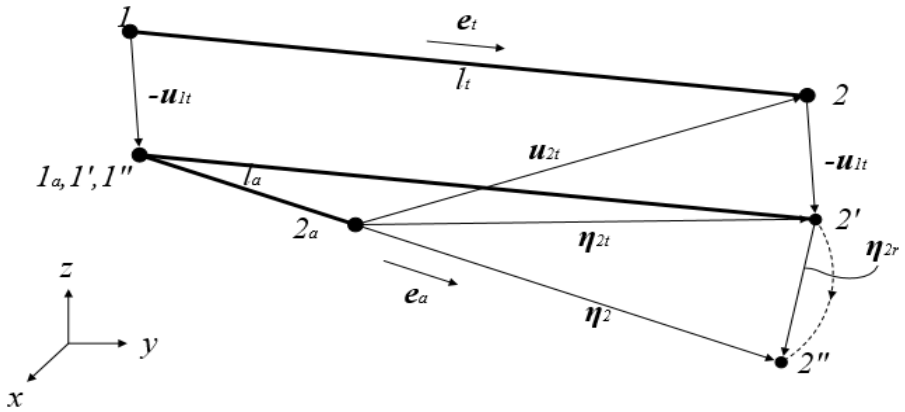

Figure 2. Reverse motion

2.3 Internal Forces

Based on the virtual inverse motion, the pure deformation of the spatial beam element in the local coordinate system is obtained, including the linear deformation, the axial deformation and the bending

ISSN: 2414-1895 DOI: 10.6919/ICJE.202107_7(7).0050

deformation , and then the axial force, torque, shear forces and bending moments of the beam element can be calculated according to the flexural theory of material mechanics.

Assuming that the node forces and bending moments of the beam element at the virtual position 1'-2' are :

$$\begin{cases} \hat{\boldsymbol{f}}^j = \begin{bmatrix} \hat{f}_1^j & \hat{f}_2^j & \hat{f}_3^j \end{bmatrix}^T \\ \hat{\boldsymbol{m}}^j = \begin{bmatrix} \hat{m}_1^j & \hat{m}_2^j & \hat{m}_3^j \end{bmatrix}^T \end{cases}, j = 1,2 \tag{13}$$

The nodal forces and bending moments of reference configuration 1a-2a are :

$$\begin{cases} \hat{\boldsymbol{f}}_a^j = \begin{bmatrix} \hat{f}_{1a}^j & \hat{f}_{2a}^j & \hat{f}_{3a}^j \end{bmatrix}^T \\ \hat{\boldsymbol{m}}_a^j = \begin{bmatrix} \hat{m}_{1a}^j & \hat{m}_{2a}^j & \hat{m}_{3a}^j \end{bmatrix}^T \end{cases}, j = 1,2 \tag{14}$$

Using the element deformation $\hat{\Delta}_e$ between nodes, the joint torsion angle $\hat{\varphi}^2{}_1$ and the rotation angle $\hat{\varphi}^1{}_2, \hat{\varphi}^2{}_2, \hat{\varphi}^1{}_3, \hat{\varphi}^2{}_3$ around the spindle plane, the internal forces and bending moments of the beam element nodes are obtained, and their expressions are :

$$\Delta\hat{f}_1^1 = -\Delta\hat{f}_1^2 = -\frac{E_a A_a}{l_a}\hat{\Delta}_e \tag{15}$$

$$\Delta\hat{f}_2^1 = -\Delta\hat{f}_2^2 = -\frac{E_a \hat{I}_{3a}}{l_a^2}(6\hat{\varphi}_3^1 + 6\hat{\varphi}_3^2) \tag{16}$$

$$\Delta\hat{f}_3^1 = -\Delta\hat{f}_3^2 = -\frac{E_a \hat{I}_{2a}}{l_a^2}(6\hat{\varphi}_2^1 + 6\hat{\varphi}_2^2) \tag{17}$$

$$\Delta\hat{m}_1^1 = -\Delta\hat{m}_1^2 = -\frac{G_a \hat{I}_{1a}}{l_a}\hat{\varphi}_1^2 \tag{18}$$

$$\Delta\hat{m}_2^1 = \frac{E_a \hat{I}_{2a}}{l_a}(4\hat{\varphi}_2^1 + 2\hat{\varphi}_2^2) \tag{19}$$

$$\Delta\hat{m}_2^2 = \frac{E_a \hat{I}_{2a}}{l_a}(2\hat{\varphi}_2^1 + 4\hat{\varphi}_2^2) \tag{20}$$

$$\Delta\hat{m}_3^1 = \frac{E_a \hat{I}_{3a}}{l_a}(4\hat{\varphi}_3^1 + 2\hat{\varphi}_3^2) \tag{21}$$

$$\Delta\hat{m}_3^2 = \frac{E_a \hat{I}_{3a}}{l_a}(2\hat{\varphi}_3^1 + 4\hat{\varphi}_3^2) \tag{22}$$

Where $\hat{I}_{1a}, \hat{I}_{2a}, \hat{I}_{3a}$ are the moment of inertia of the initial section in three directions of the principal axis; A_a and l_a are the area and length of the cross section; E_a is the tangent modulus of the axial stress; G_a is the tangent modulus of the shear stress. The above calculation is the internal forces and moments of the element in the local coordinate system, which need to be converted to the global coordinate system through the transformation matrix.

3. Numerical Model and Static Analysis

3.1 Numerical Model

Table 1. Sections and materials

Part	Section	Material
Main chord	Φ600×24 mm	JFE-HITEN780
Horizontal bar and link frame	Φ550×10 mm	A709-50-2
Oblique bar	Φ350×10 mm	Q345B

Floating crane is shaped like "A", the length between the crane root hinge points and the secondary hook is up to 112.8 m, the distance between the root two hinge points is 27 m. This model is simplified reasonably, the influence of rope deformation is ignored, and the supporting mode of the whole crane is similar to the simply supported beam. The displacement of hinge points A at the root are restricted in all three directions. The B nodes connected between the boom and the rope only limit in Z direction,

ISSN: 2414-1895 DOI: 10.6919/ICJE.202107_7(7).0050

which is used to simulate the support by rope. The load and forced displacement are applied on C points which is the position of hooks.

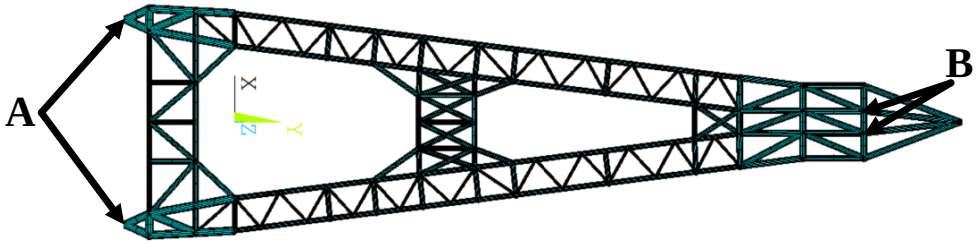

a) Top view

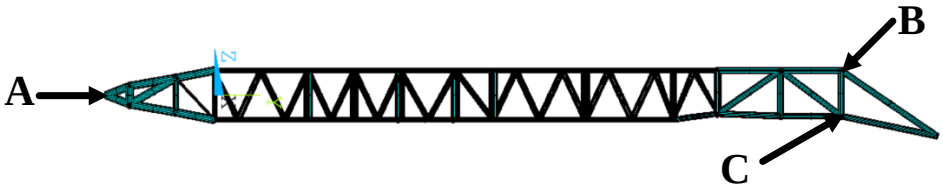

b) Side view

Figure 3. Simplified FEM modal

Modeling in Ansys, the Beam188 element is used, but the high-order shape function switch is not turned on. For the reason that the beam element in FPM adopts linear interpolation. If the high-order shape function switch is turned on, the comparison between the two results will be affected. In order to reflect the partial buckling of the beam, each beam is divided into at least two sections. Theoretically, the more the better, but computing consumes too much time and resources.

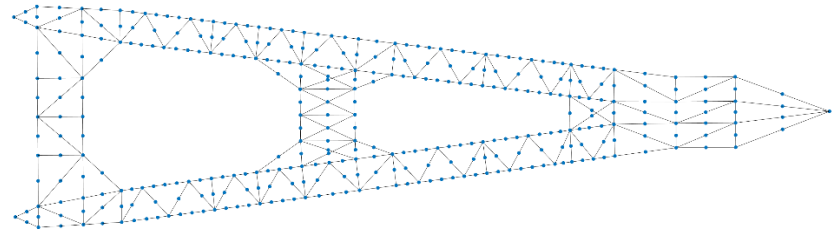

a) Top view

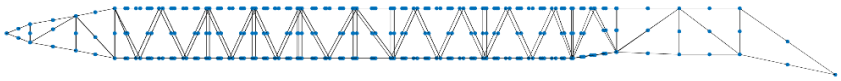

b) Side view

Figure 4. Simplified FPM modal

3.2 Static Analysis

A static analysis of the structure is carried out firstly, and vertical downward loads are applied to all nodes to simulate gravity. According to the calculation of APDL command, the maximum displacement of the boom under the gravity is 0.1678 m.

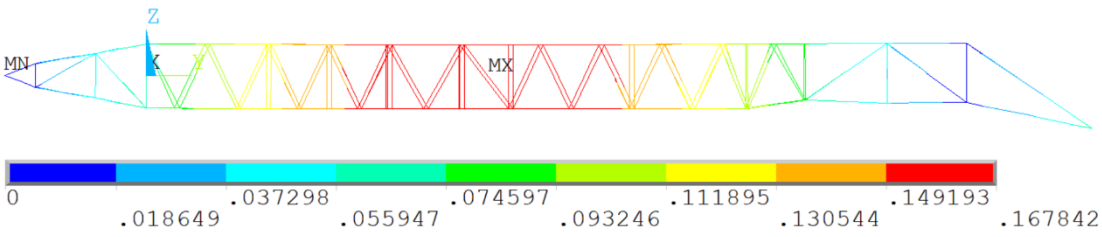

Figure 5. FEM result

ISSN: 2414-1895 DOI: 10.6919/ICJE.202107_7(7).0050

The FPM exactly adopts the same model and constraint conditions as the FEM, and the maximum displacement under deadweight load is 0.1728 m. The error between the two method is only 3%. It can be seen that the accuracy of linear calculation by FEM is high enough.

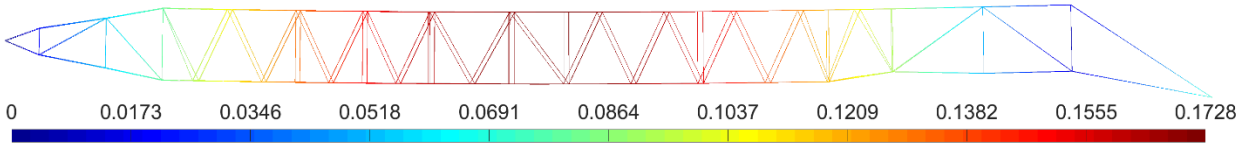

Figure 6. FPM result

4. Geometric Nonlinear Analysis

The traditional structural analysis is usually based on the theory of small displacement, and the equilibrium equation is established before the deformation. When the large displacement needs to be considered, the TL(total Lagrange) or UL(updated Lagrange) configuration is used for iterative solution or special treatment, so that the structural analysis can be divided into geometric linear problems and geometric nonlinear problems. However, the cost of geometric nonlinear analysis is much higher than that of geometric linear analysis. The explicit finite element method based on the co-rotating coordinate system can calculate the internal forces of the element in the co-rotating coordinate system, but it is difficult to separate the rigid body motion and pure deformation of the solid element, so it is still difficult to analyze the geometrical nonlinearity.

The FEM separates the rigid body motion and the pure deformation of the element through the virtual reverse motion, obtains the internal force of the element, and then restores the element to the real position after the deformation with the virtual forward motion. Therefore, it can be regarded as solving the geometric nonlinear problem in essence. Because geometric linear problems are special cases of geometric nonlinear problems, the FEM can solve geometric linear problems and geometric nonlinear problems uniformly.

In order to track the descending stage of the load, the forced displacement method is used to loading. With the initial configuration of the boom under the dead load, the nonlinear deformation of the whole structure is observed by applying a 2 m forced displacement at C point.

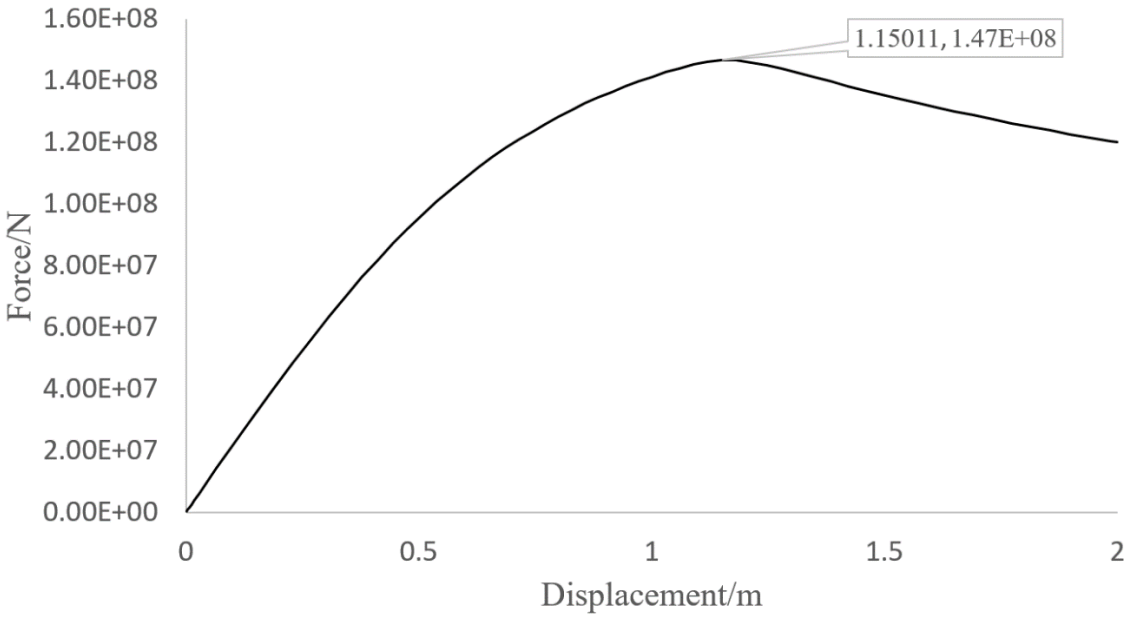

Figure 7. Load-displacement curve

ISSN: 2414-1895 DOI: 10.6919/ICJE.202107_7(7).0050

Figure 7 is a typical nonlinear curve, which belongs to the form of extreme point instability. With the forced displacement loading, the reaction force increases continuously at first.When the forced displacement is applied to 1.15 m, the ultimate load of the crane reaches 14700 t. Then across the extreme point, the bearing capacity continues to decline. The rated lifting weight of the crane is 7000 t. During its working time, the crane will also have pitch angle and load applied by the rope which is close to the lifting weight. Therefore, it is very reasonable that the axial ultimate load of the crane is more than twice of the rated lifting weight.

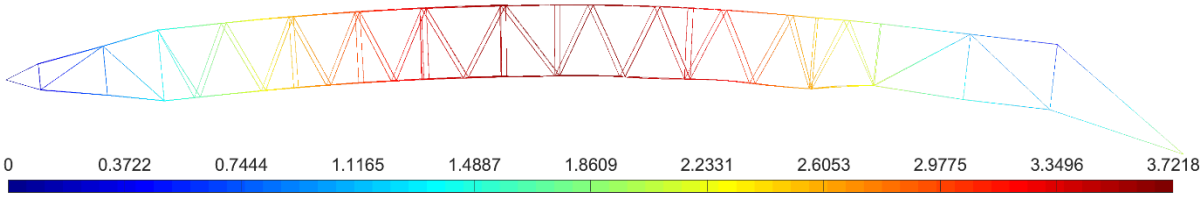

Figure 8. Deformation diagram of crane(1.15 m forced displacement)

At the time that the forced displacement is applied to 1.15 m, the crane reaches the ultimate load. Although the overall displacement is large, the partial structure can still maintain its configuration.

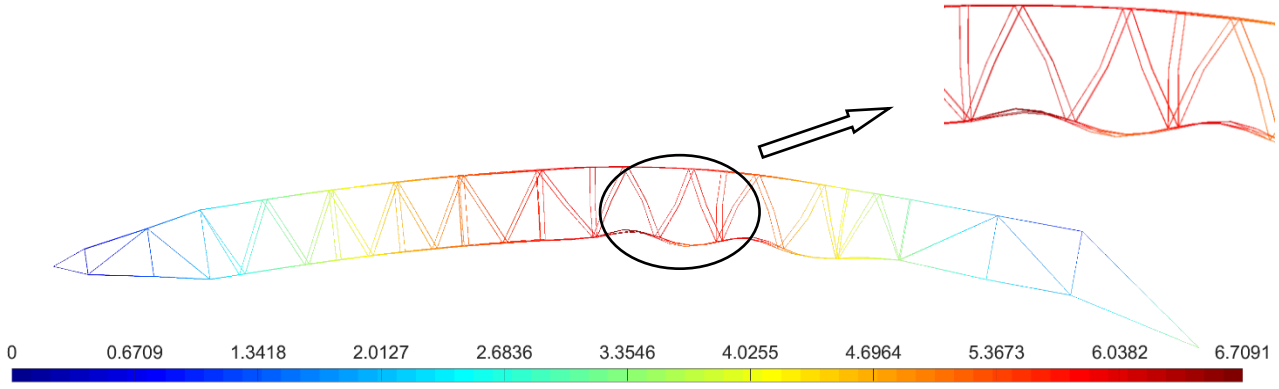

a) Side view

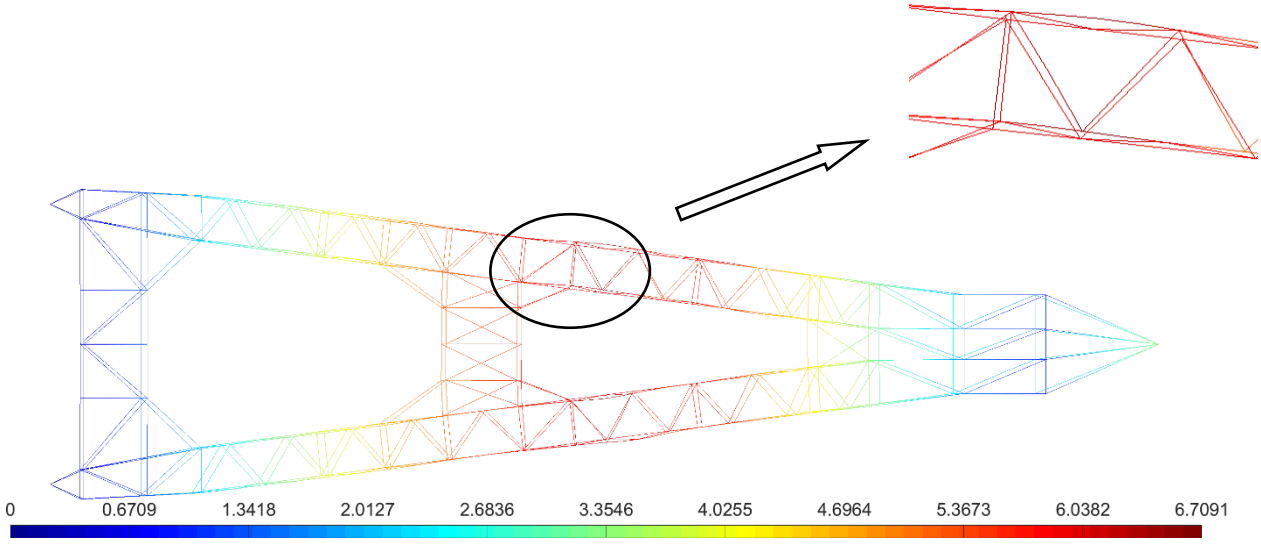

b) Top view

Figure 9. Deformation diagram of crane(2 m forced displacement)

When the forced displacement is applied to 2 m, the partial bar also deforms obviously. The deformation of the bar above the link frame is particularly serious, and the chord and oblique bar all have obvious lateral displacement.

ISSN: 2414-1895 DOI: 10.6919/ICJE.202107_7(7).0050

By analyzing the whole process of the crane instability, we can found that it presents the characteristics of overall instability first and then local instability during the loading process. The ultimate load of the boom mainly depends on the design of the whole structure, and the strength of the partial bar is high enough before the extremum point. After the extremum point is passed, partial buckling begins to occur.

5. Conclusion

Researching on the 7000 t floating crane, the FPM is used to study its geometric nonlinearity. The accuracy and efficiency of FPM is strongly verified by static analysis. The load-displacement curve of the structure was obtained by the forced displacement method, and the accurate ultimate load was obtained. According to the buckling deformation form of the crane under load, the main parts and specific process of the crane instability could be evaluated, and the parts with large deformation and partial instability could be strengthened and optimized.

However, the whole analysis process is based on the elastic deformation of the structure without introducing the elastoplastic constitutive of the material. The plastic deformation has a great influence on the post-buckling strength of the structure, which needs to be further studied. In addition, the local analysis is not detailed and comprehensive, and the subsequent consideration is to extract the local bar separately for research, so as to more clearly define the relationship between the global and the local instability.

Acknowledgments

Innovation Action Plan Projects of Shanghai Science and Technology Commission (18DZ1100802).

References

[1] Yurchenko D., Alevras P. Stability of a stochastic ship crane. Safety, Reliability, Risk and Life-Cycle Performance of Structures and Infrastructures-Proceedings of the 11th International Conference on Structural Safety and Reliability, Vol. 16 (2013), p. 1115-1120.

[2] Jung Hoon-Hyung, Kim Chae-Sil. A study on the stability of a mast structure for erecting a large crane. Applied Mechanics and Material, Vol. 110(2012), p. 1483-1490.

[3] Wenjun Li, Jiong Zhao, Zhen Jiang, Wei Chen,Qicai Zhou. A numerical study of the overall stability of flexible giant crane booms. Journal of Constructional Steel Research, Vol. 105(2015), p. 12-17.

[4] Simao Pedro D., Girao Coelho Ana M.,Bijlaard Frans S.K..Stability design of crane columns in mill buildings. Engineering Structures, Vol. 42(2021), p. 51-82.

[5] Jia Yao, Xiaoming Qiu, Zhenping Zhou, Yuqin Fu, Fei Xing, Erfei Zhao. Buckling Failure analysis of all-terrain crane telescopic boom section. Engineering Failure Analysis, Vol. 57(2015), p. 105-117.

[6] Frendo Francesco. Analysis of the catastrophic failure of a dockside crane jib. Engineering Failure Analysis, Vol. 31(2013), p. 394-411.

[7] Ding Chengxian, Duan Yuanfeng,Wu Dongyue. Vector Mechanics of Structures (Science Press, China 2012).

[8] Luo Yaozhi, Yu Ying. Finite particle method for structural complex behavior analysis (Science Press, China 2019).

[9] Yan Zhang, Deshen Chen, Hongliang Qian. Computational method for the deformation mechanism of non-prestressed cable net structures based on the vector form intrinsic finite element method. Engineering Structures, Vol. 231(2021), p. 1-11.

[10] Ying Yu, Xingyi Zhu. Nonlinear dynamic collapse analysis of semi-rigid steel frames based on the finite particle method. Engineering Structures, Vol. 118(2016), p. 383-393.

[11] Yulong Yang, J. J. Roger Cheng, Tuqiao Zhang. Vector form intrinsic finite element method for planar multibody systems with mutiple clearance joints. Nonlinear Dynamics, Vol. 86(2016), p. 421-440.

ISSN: 2414-1895 DOI: 10.6919/ICJE.202107_7(7).0050

[12] Jingzhe Tang, Yanfeng Zheng, Chao Yang, Wei wang, Yaozhi Luo. Parallelized implementation of the finite particle method for explicit dynamics in GPU. Computer Modeling in Engineering&Sciences, Vol. 122(2020), p. 5-31.

[13] Feihong Liu, Ying Yu, Qinhua Wang, Yaozhi Luo.A coupled smoothed particle hydrodynamic and finite particle method: An efficient approach for fluid-solid interaction problems involving free-surface flow and solid failure. Engineering Analysis with Boundary Elements, Vol. 118(2020), p. 143-155.

[14] Yuanfeng Duan, Junjie Tao, Hongmei Zhang, Sumei Wang, Chungbang Yun.Real-time hybrid simulation based on vector form intrinsic finite element and field programmable gate array. Structural Control and Health Monitoring, Vol. 26(2019), p. 1-21.